



HAL
open science

Radiotherapy-Related Gene Signature in Prostate Cancer

Sotirios Fortis, Maria Goulielmaki, Nicolas Aubert, Panagiota Batsaki, Sotirios Ouzounis, Dionisis Cavouras, Gilles Marodon, Savvas Stokidis, Angelos Gritzapis, Constantin Baxevanis

► **To cite this version:**

Sotirios Fortis, Maria Goulielmaki, Nicolas Aubert, Panagiota Batsaki, Sotirios Ouzounis, et al.. Radiotherapy-Related Gene Signature in Prostate Cancer. *Cancers*, 2022, 14 (20), pp.5032. 10.3390/cancers14205032 . inserm-03841361

HAL Id: inserm-03841361

<https://inserm.hal.science/inserm-03841361v1>

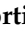



Submitted on 7 Nov 2022

HAL is a multi-disciplinary open access archive for the deposit and dissemination of scientific research documents, whether they are published or not. The documents may come from teaching and research institutions in France or abroad, or from public or private research centers.

L'archive ouverte pluridisciplinaire **HAL**, est destinée au dépôt et à la diffusion de documents scientifiques de niveau recherche, publiés ou non, émanant des établissements d'enseignement et de recherche français ou étrangers, des laboratoires publics ou privés.

Article

Radiotherapy-Related Gene Signature in Prostate Cancer

Sotirios P. Fortis¹, Maria Goulielmaki¹ , Nicolas Aubert², Panagiota Batsaki¹, Sotirios Ouzounis^{3,4} ,
Dionisis Cavouras³, Gilles Marodon² , Savvas Stokidis¹, Angelos D. Gritzapis¹
and Constantin N. Baxevanis^{1,*} 

¹ Cancer Immunology and Immunotherapy Center, Cancer Research Center, Saint Savas Cancer Hospital, 11522 Athens, Greece

² Centre d'Immunologie et Maladies Infectieuses-Paris, CIMI-PARIS, Sorbonne Université, INSERM, CNRS, 75013 Paris, France

³ Department of Biomedical Engineering, University of West Attica, 12243 Athens, Greece

⁴ Institute of Chemical Biology, National Hellenic Research Foundation, 11635 Athens, Greece

* Correspondence: costas.baxevanis@gmail.com; Tel.: +30-21-0640-9380

Simple Summary: Radiation therapy (RT) is an established therapeutic regimen for prostate cancer patients which aims for the direct elimination of tumor cells in the prostate gland and occasionally at distant anatomic sites. In this study, we performed next-generation sequencing-based gene expression analysis in peripheral blood from prostate cancer patients obtained pre- and post-radiotherapy and found six independently down-regulated genes including *CCR7*, *FCGR2B*, *BTLA*, *CD6*, *CD3D*, and *CD3E*. The analysis of the expression of the 6-genes as a signature also revealed significantly lower levels post- vs. pre-radiotherapy. Data extracted from the PRAD (PRostate ADenocarcinomas) dataset linked low levels of the 6-gene signature to better survival. More importantly, this 6-gene signature strongly correlated with a favorable prognosis regardless of poor standard clinicopathological parameters (i.e., Gleason score ≥ 8 and T3), thus highlighting its potential predictive value.



Citation: Fortis, S.P.; Goulielmaki, M.; Aubert, N.; Batsaki, P.; Ouzounis, S.; Cavouras, D.; Marodon, G.; Stokidis, S.; Gritzapis, A.D.; Baxevanis, C.N. Radiotherapy-Related Gene Signature in Prostate Cancer. *Cancers* **2022**, *14*, 5032. <https://doi.org/10.3390/cancers14205032>

Academic Editors:
Bartosz Małkiewicz and
Jakub Dobruch

Received: 15 September 2022

Accepted: 11 October 2022

Published: 14 October 2022

Publisher's Note: MDPI stays neutral with regard to jurisdictional claims in published maps and institutional affiliations.



Copyright: © 2022 by the authors. Licensee MDPI, Basel, Switzerland. This article is an open access article distributed under the terms and conditions of the Creative Commons Attribution (CC BY) license (<https://creativecommons.org/licenses/by/4.0/>).

Abstract: Radiotherapy for localized prostate cancer has increased the cure and survival rates of patients. Besides its local tumoricidal effects, ionizing radiation has been linked to mechanisms leading to systemic immune activation, a phenomenon called the abscopal effect. In this study, we performed gene expression analysis on peripheral blood from prostate cancer patients obtained post-radiotherapy and showed that 6 genes, including *CCR7*, *FCGR2B*, *BTLA*, *CD6*, *CD3D*, and *CD3E*, were down-regulated by a range of 1.5–2.5-fold as compared to pre-radiotherapy samples. The expression of the signature consisting of these six genes was also significantly lower post- vs. pre-radiotherapy. These genes are involved in various tumor-promoting immune pathways and their down-regulation post-radiotherapy could be considered beneficial for patients. This is supported by the fact that low mRNA expression levels for the 6-gene signature in the prostate tumor tissue was linked to better survival. Importantly, we report that this 6-gene signature strongly correlated with a favorable prognosis regardless of poor standard clinicopathological parameters (i.e., Gleason score ≥ 8 and T3 (including T3a and T3b)). Our pioneering data open the possibility that the 6-gene signature identified herein may have a predictive value, but this requires further long-term studies.

Keywords: prostate cancer; radiotherapy; immune system; gene-expression; six-gene signature; predictive biomarker

1. Introduction

Targeted therapeutics constitute a major part among multifaceted cancer treatments [1]. Such targeted therapies among others may also involve immune checkpoint or kinase inhibitors which act to activate antitumor immune reactivity either directly by reinvigorating the exhausted endogenous antitumor immunity or indirectly by neutralizing over-activated oncogenic pathways [2,3]. These agents may have a greater impact on clinical outcomes

if combined with treatment modalities that down-regulate the expression of immune suppressor genes.

Although prostate cancer (PCa) has survival rates of more than 90% after 5 years, it is still one of the major causes of cancer-related death among men in western countries due to its high incidence [4]. Radiation therapy (RT) is an established treatment option for the management of localized PCa (LPCa) [5], which aims to directly kill tumor cells in the prostate gland and occasionally at distant anatomic sites [6]. There is accumulating evidence to suggest that RT generates local and also systemic immune-based pathways variously [7,8], but mostly via the release of tumor antigens which are specifically recognized by T cells and induce downstream signaling [9–11]. However, so far, there is no report on the identification of genes that are affected by RT and are involved in immune activation mechanisms controlling tumor progression. Therefore, the present study aimed to investigate the alterations in immune response genes in the peripheral blood of PCa patients with localized disease post-RT, and to analyze the correlation of these changes with the incidence of recurrences from the Prostate Adenocarcinoma (PRAD) dataset. Thus, the potential mechanisms of immune activation induced by RT might be clarified, which may improve our understanding of tumor immune surveillance.

2. Materials and Methods

2.1. Selection of Patients and Samples

Twenty-three PCa patients were enrolled between 1/2019–6/2020. The clinicopathological characteristics are summarized in Table 1. All the patients had acinar adenocarcinoma of the prostate. Seventeen patients received primary RT, while the remainders ($n = 6$) received RT post-radical prostatectomy (adjuvant RT). Only the patients who completed the radiation schedule without breaks or dose reductions were eligible for the study. All six patients who were treated with adjuvant RT after radical prostatectomy had positive margins. Second, all patients who were treated with primary RT ($n = 17$) or adjuvant RT after radical prostatectomy ($n = 6$) were already under androgen-deprivation therapy (ADT) during the past six months (and therefore at the first blood sampling (i.e., pre-RT)).

Table 1. Clinicopathological characteristics of the patients and details of the radiation therapy.

Patients with Localized PCa (n = 23)	
Characteristics of Initial PCa Staging	
Median Age at Diagnosis (Years) (Range)	73 (53–81)
PSA	
Mean	18.74 ng/mL
SD	20.85 ng/mL
Range	5.51–100.00 ng/mL
Gleason Score	
Mean	7
SD	1
Range	6–9
T	
T1c	3 (13.0%)
T2a, T2b, T2c	12 (52.2%)
T3a, T3b	8 (34.8%)
Type of radiation therapy	
Primary	17 (73.9%)
Adjuvant	6 (26.1%)
External beam radiation therapy (EBRT) characteristics	
3D Conformal Radiotherapy	
Median daily dose; Gy (range)	2 (1.8–2.2)
Median total dose; Gy (range)	70 (66–72)
Median Radiation treatment schedule; days (range)	37 (35–38)

Blood was collected before the initiation of RT and 90 days after the end of RT. The blood sampling was performed by the medical doctor and the blood was collected in a tube containing K2E (EDTA). This time point (i.e., 3 months) was chosen based on previous findings, reporting that by this time the immune cell populations have recovered to their normal numbers before the initiation of therapy [12,13]. Patient follow-up ranged between 22 and 39 months depending on the patient's enrolment date.

2.2. Ethics Approval

The study was conducted in accordance with the Declaration of Helsinki, and all of the participants provided written informed consent. The study was approved by the Saint Savas Cancer Hospital Institutional Review Board (approval no. IRB-ID6777/14-06-2017) and the Ethical Committee of the Medical School of the National and Kapodistrian University of Athens (approval no. ID247/28-01-2020).

2.3. Isolation of RNA

RNA was extracted from peripheral blood using the PureLink™ Total RNA Blood Kit (Invitrogen, ThermoFisher, Waltham, MA, USA) within thirty minutes after the blood collection. As a next step, we performed DNase treatment using ezDNase™ Enzyme (Invitrogen, ThermoFisher, Waltham, MA, USA) to ensure that there were no contaminations with DNA. The quantification of the extracted RNA was performed by a Qubit Fluorometer 3.0 (ThermoFisher, Waltham, MA, USA), which detects fluorescent dyes specific to the RNA. The quantity of the input was 10 ng of total RNA, which was used for manual library preparation. The extracted RNA was stored at -80°C .

2.4. Oncomine Immune Response Research Assay

The RNA-based Next Generation Sequencing (NGS) panel Oncomine Immune Response Assay (OIRRA) (ThermoFisher, Waltham, MA, USA) was adopted to measure the expression levels of immune-related genes. This panel allowed the simultaneous evaluation of 398 genes related to immune system activation, including genes associated with adhesion, migration, TCR co-expression, checkpoint pathways, cytokine signaling, dendritic cells, macrophage, lymphocyte infiltrate, and B cell markers. The RNA-sequencing analysis was performed on RNA from the peripheral blood of the patients. In detail, cDNA synthesis was performed using SuperScript™ VILO™ cDNA Synthesis Kit (Invitrogen, ThermoFisher, Waltham, MA, USA) for the preparation of cDNA target amplification reactions. For library preparation, Ion AmpliSeq™ Library Kit 2.0 (Ion Torrent™, ThermoFisher, Waltham, MA, USA) and Ion Xpress™ Barcode Adapters (Ion Torrent™, ThermoFisher, Waltham, MA, USA) were used and AMPure XP (Beckman Coulter, Brea, CA, USA) beads were employed for purification and size selection throughout the workflow. Subsequently, qPCR was performed for library quantification, using an Ion Library TaqMan™ Quantitation Kit (Ion Torrent™, ThermoFisher, Waltham, MA, USA) and a Quantstudio 5.0 Real-Time PCR instrument and software (ThermoFisher, Waltham, MA, USA). The concentration per library was 50 pM for Ion Chef Preparation and after dilution and calculation of the proper concentration, the libraries were combined in order to proceed with templating and sequencing. Template preparation and chip loading took place on the Ion Chef System (ThermoFisher, Waltham, MA, USA) and the sequencing step was executed using the Ion S5 System (ThermoFisher, Waltham, MA, USA). The targeted RNA-sequencing analysis was obtained using the Ion Torrent Immune Response RNA plugin that produced gene transcript data.

2.5. Gene Expression Analysis and Statistics

The Read Per Million data (RPM) were log-transformed and normalized and the gene-level count data generated from the run were further analyzed with the Affymetrix Transcriptome Analysis Console (TAC) software. Results normalized by RPM were downloaded from the Immune Response RNA plugin and then uploaded to the TAC software.

The Read cutoff per sample was 1.5 million total reads. Gene expression analysis and graph preparation were performed in GraphPad Prism 8.0.2 for Windows (GraphPad Software, Inc., San Diego, CA, USA), using the normalized average log₂ values corresponding to gene expression levels, as well as the resulting fold change values. A non-parametric Wilcoxon's (paired) test was performed for the identification of differences in immune gene expression among patients pre- and post-RT. Data are presented as the median with range. A correlation matrix analysis (Pearson coefficient) was used to compute the correlation between the six genes that constitute the proposed signature, before and post-RT. P values below 0.05 were considered to indicate a statistically significant difference. The interaction network of the 6-GS was built using the GeneMANIA database [14]. Accordingly, the interaction network of the respective proteins was built using the STRING database [15]. Gene Ontology was conducted using the GOnet tool, available from [16]. Univariate and multivariate survival analyses (Cox regression) were conducted using IBM SPSS 24 (SPSS Inc., Chicago, IL, USA). For the multivariate analysis, the forward stepwise method with a threshold of 0.05 as an entry point was used. All categorical covariates were transformed into numeric codes as follows: GS: ≤ 6 , 1; 7, 2; ≥ 8 , 3; T status: T1-T2, 1; T3, 2; 6-gene signature: Low expression, 1; High expression, 2.

2.6. TCGA PRAD Analysis

The PRAD data from The Cancer Genome Atlas (TCGA) database were extracted using the Xena browser (<http://xena.ucsc.edu>, accessed on 15 July 2022) provided by the University of California (Santa Cruz, CA, USA). mRNA expression of genes of interest, progression-free interval (PFI), PFI-time and phenotypic data were used (sample_type, pathologic_T-stage, Gleason_score and PSA value). Only primary tumor samples (n = 497) were selected for subsequent analysis. A patient was considered with a high gene expression if the expression level of this was higher than its respective median among all PRAD patients. Otherwise, a patient was considered with a low expression. Then, additional genes of interest were sequentially added to the primary analysis leading to the 6-GS.

3. Results

3.1. Sample Demographics

Twenty-three patients with LPCa undergoing external beam radiation therapy (EBRT) were enrolled in the study (Table 1). The mean age of the subjects was 73 [range, 53–81] years. Almost half of the patients (n = 12/23; 52.2%) had stage T2 (a–c) disease with Gleason scores ranging from 6 to 9 (mean: 7) and baseline PSA mean levels 18.74 ng/mL (range, 5.51–100.00 ng/mL) that were consistent with intermediate- to high-risk progression of the disease (Table 1) [17]. Seventeen of the participants were receiving primary RT and the remaining six patients had adjuvant RT post radical prostatectomy. The EBRT characteristics are presented in Table 1. Notwithstanding the two groups receiving different treatments, we should note that biochemical control rates in patients with localized PCa treated either with ERBT or with RP appear similar over extended periods of time [18,19]. This would suggest that the tumor burden in these two groups is either similar or, if with minor differences, these should not interfere with molecular or phenotypical alterations in peripheral blood. Therefore, we analyzed the data from these 2 groups jointly.

3.2. Gene Expression and Survival

Six genes related to (a) immune checkpoints (n = 2; *BTLA* and *CD6*); (b) regulatory macrophages and T cells (n = 2; *CCR7* and *CD3D*); and (c) immune deficiencies and unfavorable prognosis (n = 2; *CD3E* and *FCGR2B*) were down-regulated post-RT compared with pre-RT (statistical *p*-range: <0.0001–0.0415; Figure 1).

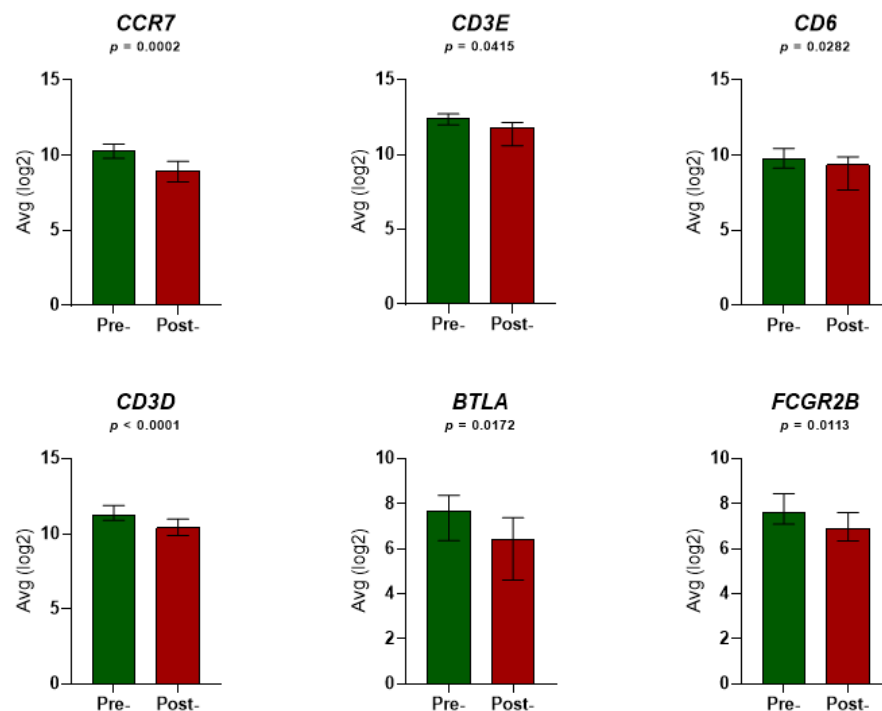


Figure 1. Expression levels of the six immune-related genes in the peripheral blood of 23 localized prostate cancer (LPCa) patients before and after radiation therapy (RT). Each graph corresponds to expression level alterations of each single gene pre-RT and post-RT. Each column illustrates the average mRNA levels of each gene normalized by RPM and log₂-transformed. Non-parametric Wilcoxon's (paired) test was performed to indicate whether the expression levels pre-RT and post-RT differed significantly among patients. The error bars denote the median values with interquartile range. P values below 0.05 indicate statistical significance. Avg: average.

Four of the six genes (*BTLA*, *CCR7*, *CD6* and *CD3D*) were between 2.0-fold and 2.5-fold down-regulated, whereas *FCGR2B* and *CD3E* were down-regulated by 1.56-fold and 1.45-fold, respectively (Figure 2A). Moreover, the 6-genes jointly analyzed as a signature, were expressed at significantly lower levels post-RT vs. pre-RT ($p < 0.0001$; Figure 2B). The heat map demonstrated the differential gene expression levels in the two time-periods (Figure 2C).

Due to the extended time-period required for survival analyses in patients with LPCa [20], we explored the clinical significance of our data using the PRAD dataset. In this database, information from 498 primary tumor samples is available for analysis. For one patient there were no follow-up data. Of the remaining 497 patients, only three patients (<1%) had confirmed metastatic disease. Thus, the PRAD-cohort including almost entirely patients with localized disease was comparable to our group.

We compared PFI in LPCa patient groups stratified by the 6-GS levels in prostate tumor tissue above vs. below median (simulating the higher vs. decreased expression levels of this signature in patients' peripheral blood at pre-RT and post-RT, respectively). As shown in Figure 3A, PFI was significantly higher in the group of patients with levels of the 6-GS below median vs. those expressing 6-GS levels above median. We next examined survival in PCa patients with poor prognosis based on standard clinicopathological parameters including patients with Gleason score ≥ 8 and T-stage T3. Also, in this case, PFI was markedly higher in patients with the 6-GS expression levels below median than above median (Figure 3B,C).

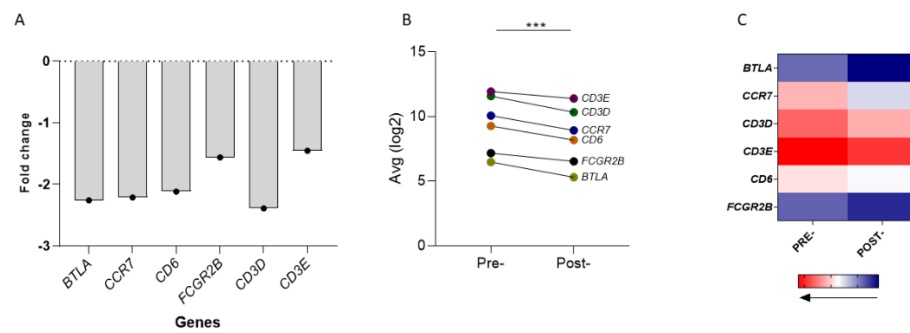


Figure 2. Alterations in gene expression of the 6-GS in the peripheral blood of 23 LPCa patients before and after RT. (A) Scatter dot plot representing fold change (FC) in the six genes pre-RT and post-RT. FC values were generated by conversion of the normalized average log2 values corresponding to gene expression levels pre-RT and post-RT. Data are presented as means. (B) The 6-GS is significantly downregulated post-RT (** $p < 0.0001$). The depicted lines represent the conversion of each described gene from higher (pre-RT) to lower levels (post-RT). (C) Heat map showing the range of differential expression levels of the six genes. For the analysis, the median expression levels of each gene, pre-RT and post-RT, were used. The expression level values were normalized by RPM, log2-transformed and then median-centered for each patient. Different colors indicate different levels of gene expression: from red (high expression, max. value 12.43) to blue (low expression, min. value 6.42).

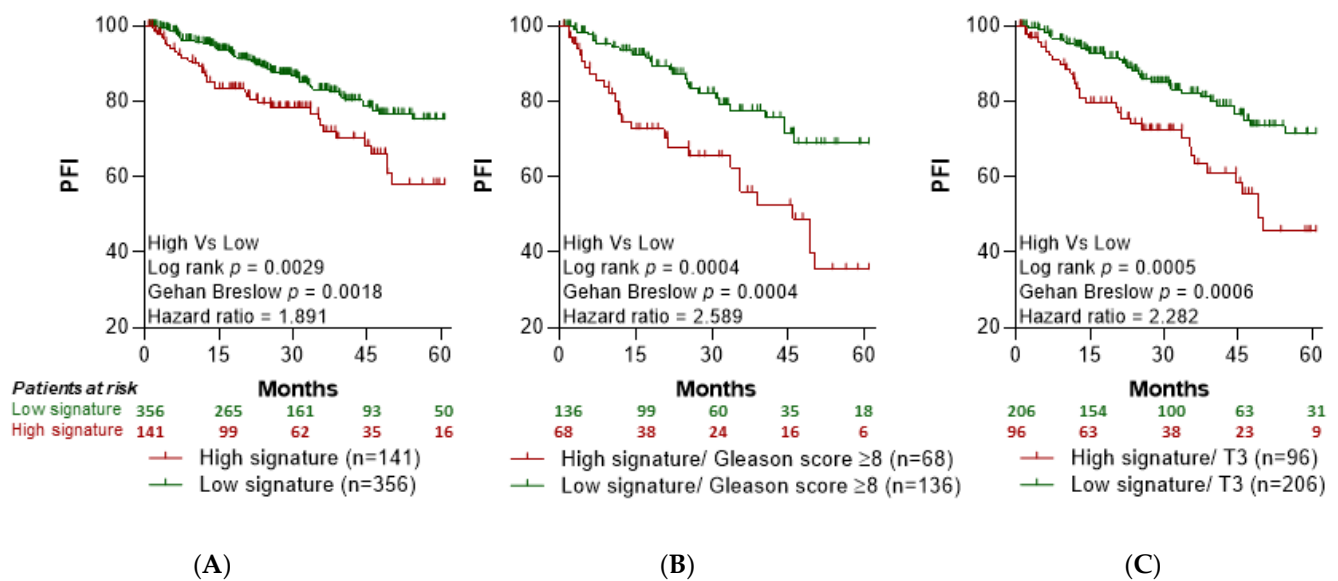


Figure 3. The 6-GS is associated with lower progression-free intervals in PCa patients. Kaplan-Meier curves for Progression Free Interval (PFI) in PCa patients were designed based on the dichotomized median expression of the 6-GS in prostate tumor tissue. (A) Association between the 6-GS expression levels and PFI in PCa patients. (B) Association between the 6-GS expression levels and PFI among PCa patients with Gleason score ≥ 8 . (C) Association between the 6-GS expression levels and PFI among PCa patients with T3 (3a,3b) stage tumors. The data were extracted from the PRAD (PRostate ADenocarcinomas) dataset. The red lines indicate cases with high expression (expression value $>$ median), while the green lines indicate cases with low expression (expression value $<$ median) of the 6-GS. Moreover, the number of patients at risk are presented in the graph.

Importantly, PFI for patients with high risk of recurrence based on the standard clinicopathological parameters (i.e., T3 or Gleason score ≥ 8) but having the 6-GS levels below median, did not statistically differ from PFI observed in patients with more favorable clinicopathological parameters (i.e., Gleason score = 7 or T2; Figure 4A,B, respectively).

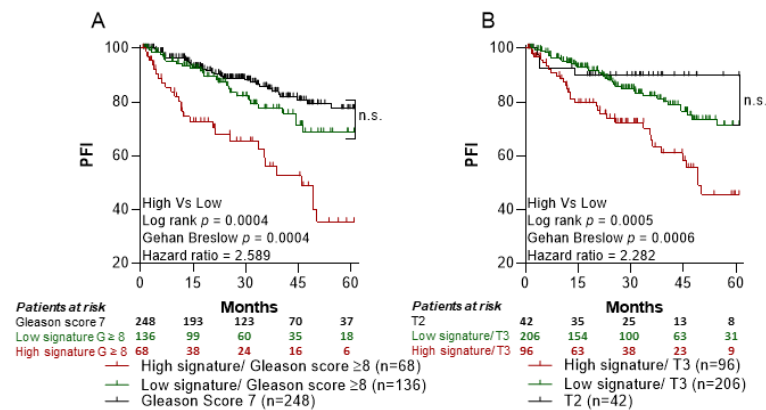


Figure 4. Prognostic potential of the 6-GS in PCa patients. Kaplan-Meier curves for Progression Free Interval (PFI) were designed based on the median expression of the 6-GS in prostate tumor tissue in association with poor clinicopathological parameters. Moreover, the number of patients at risk are presented in the graph. (A) No significant difference in PFI among patients with high Gleason score (≥ 8) and low expression (below median) of the 6-GS (green line; $n = 136$) and patients with intermediate Gleason score (7) (black line; $n = 248$). In the same lines, (B) the PFI in the group of patients with unfavorable T3 stage (3a,3b) and low expression of the 6-GS (green line, $n = 206$) did not differ statistically as compared to PFI in patients with more favorable T2 stage (2a–2c) (black line, $n = 42$). Patients with high expression of the 6-GS (above median) having either Gleason score ≥ 8 (A) or T3 stage (3a,3b) (B) (red lines; $n = 68$ and $n = 96$ for A and B, respectively) had a significantly worse PFI as compared to patients with low expression of the 6-GS (green lines). n.s.: non significance.

To investigate the prognostic significance of the 6-GS, we conducted univariate and multivariate analyses in the results extracted from the PRAD database, using established clinicopathological factors (i.e., Gleason score and T stage) and our 6-GS as covariates and 5-years PFI as endpoint. In the univariate analysis (Table 2), a statistically strong impact for the patients expressing high levels of the 6-GS ($p = 0.003$) on PFI was revealed. In addition, the statistical significance of the 6-GS was stronger than the T stage ($p = 0.005$). In the multivariate analysis, the prognostic significance of the three covariates (T stage, Gleason score and 6-GS) was analyzed (Table 2). After stepwise selection, the 6-GS was found to be a strong prognosticator for the PFI ($p = 0.006$). However, as expected, the Gleason score remained a stronger prognostic factor ($p < 0.001$).

Functional networks of the six differentially expressed genes were examined to determine the involved pathways. The network analysis describes pathways that are related to (1) regulation of leukocyte cell-cell adhesion and regulation of T-cell activation; (2) leukocyte cell-cell adhesion; (3) positive regulation of cell-cell adhesion and positive regulation of leukocyte cell-cell adhesion; (4) positive regulation of cell, leukocyte, lymphocyte and T-cell activation; (5) lymphocyte co-stimulation; (6) antigen receptor-mediated signaling pathway; and (7) receptor complex function (Figure 5A). The most important linkage was found between *TNFRSF14* (*HVEM*) and the 6-GS (through *BTLA*). We also investigated the internal interactions of RT-downregulated gene products by mapping them to the PPI network using the STRING database [15]. The minimum required interaction score was set at 0.400 (medium confidence). The results showed that CD3E had the strongest correlation with the majority of the other gene products, followed by CD3D and CCR7 (Figure 5B). More specifically, the analysis revealed an average node degree (average number of edges per node) of 2.67, with an average local clustering coefficient (strength of the connection between adjacent nodes, ranging between 0 and 1) of 0.75 and a PPI enrichment p -value of 1.23×10^{-9} (significance of interactions). These parameters indicate that the resulting network has significantly more interactions than would be expected for a random set of proteins of the same size and degree of distribution. Text-mining interactions and co-expression were revealed between certain proteins (CD6/CD3D, CD3D/CD3E, CD6/CD3E, CD3E/FCGR2B, CD3E/CCR7, CD3D/CCR7, FCGR2B/CCR7, CCR7/BTLA). Figure 6 shows the six downregulated genes and the functional groups (GO

term/pathway nodes) they relate to. The respective *p*-values and gene interconnections are shown in Table S1.

Table 2. Univariate and multivariate survival analyses (Cox regression) were conducted by IBM SPSS 24. For the multivariate analysis, the forward stepwise method with a threshold of 0.05 as an entry point was used.

Univariate	PFI		
	<i>p</i>	Hazard Ratio	HR (95.0% CI)
T status	0.005	2.032	1.233–3.349
Gleason Score	<0.001	2.389	1.621
6-gene Signature	0.003	1.891	1.234–2.898
Multivariate	PFI		
	<i>p</i>	Hazard Ratio	HR (95.0% CI)
Model Before Stepwise Selection			
T status	0.312	1.324	0.768–2.281
Gleason Score	<0.001	2.137	1.405–3.250
6-gene Signature	0.007	1.808	1.179–2.772
Model after Stepwise Selection			
Gleason Score	<0.001	2.337	1.588–3.439
6-gene Signature	0.006	1.828	1.193–2.802

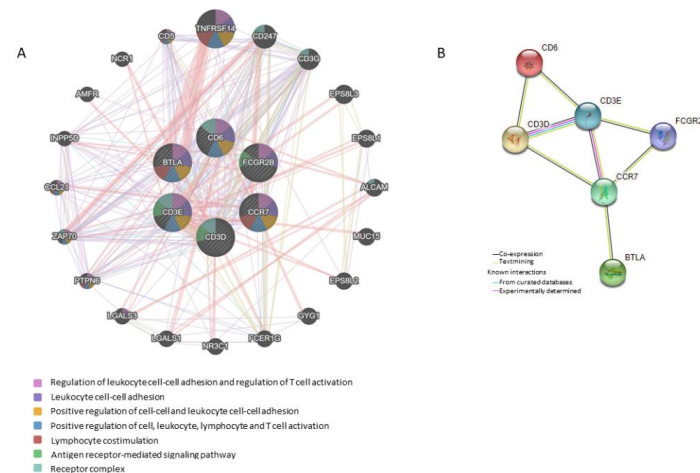


Figure 5. Functional network analysis of the six differentially expressed genes post-RT in LPCa patients. (A) Gene interaction network built on the 6-GS using the GeneMANIA database. The different color of the lines connecting the relevant genes depicts the type of interaction, including (1) regulation of leukocyte cell-cell adhesion and regulation of T-cell activation; (2) leukocyte cell-cell adhesion; (3) positive regulation of cell-cell adhesion and positive regulation of leukocyte cell-cell adhesion; (4) positive regulation of cell, leukocyte, lymphocyte and T-cell activation; (5) lymphocyte co-stimulation; (6) antigen receptor-mediated signaling pathway; and (7) receptor complex function. (B) Internal interactions between the 6-GS expression products. The corresponding proteins were mapped in the protein-protein interaction (PPI) network using the STRING database. Nodes and edges represent proteins and their interactions, respectively. Filled, colored nodes represent query proteins and first shell of interactors with known or predicted 3D structures. Turquoise and pink edges show known interactions extracted from curated databases or those experimentally determined, respectively. Yellow edges represent text-mining interactions, black edges indicate that the respective proteins are co-expressed.

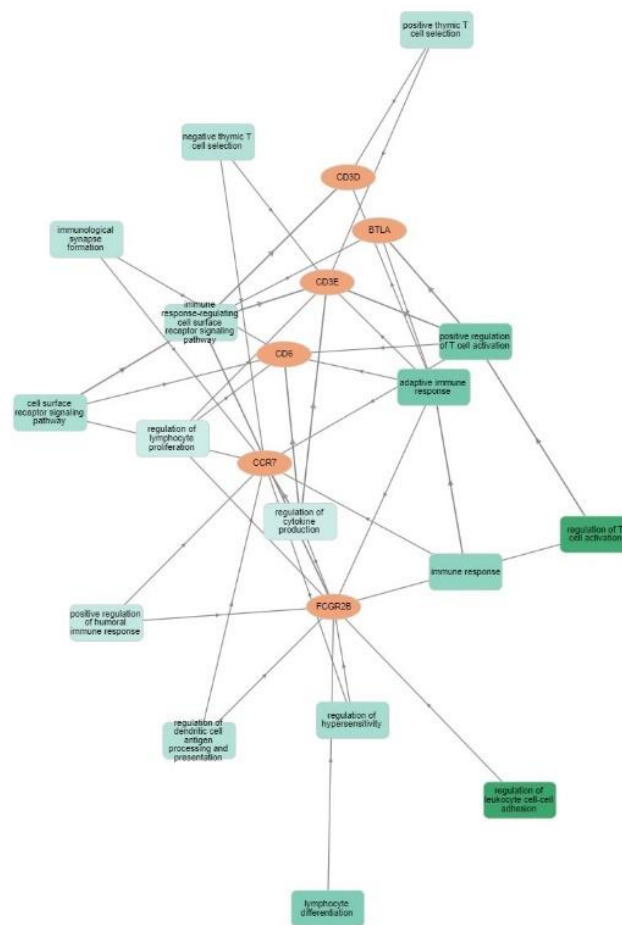


Figure 6. Visualization of Gene Ontology (GO) enrichment profiles of the 6-gene signature using the GOnet tool (only gene-connected terms, p -value threshold $\leq 7.22 \times 10^{-5}$). The orange-colored nodes represent the 6 downregulated genes, while the green-colored nodes represent the functional groups (GO term/pathway nodes). The GO term/pathway network connectivity is defined by edges. GO term/pathway nodes are colored according to p -value of enrichment. The dark green nodes show higher statistical significance than the light green nodes (regulation of leukocyte cell-cell adhesion; p -value = 4.10×10^{-6} and inflammatory response; p -value = 2.88×10^{-1} , respectively).

4. Discussion

Novel platforms are emerging as valuable tools for the diagnosis, longitudinal patient monitoring and disease prognosis, as well as for the prediction of response to treatment. Among these, the stable adoption of liquid biopsy, novel immunohistochemical assays and gene-related signatures seem to be promising across urological malignancies. For example, the qualitative and quantitative characterization of circulating tumor cells (CTCs) identified by liquid biopsy has been proven more reliable than PSA in predicting the survival of metastatic prostate patients [21] while the size of the tumor fraction in cell-free DNA is related to disease staging and tumor burden [22]. In patients with bladder cancer, quantification of CTCs before radical cystectomy can be a strong prognosticator of disease recurrence and overall survival [23]. Moreover, as recently reviewed by Casanova-Salas et al., CTCs genetic profiling holds strong predictive potential for the identification of responders among prostate patients that receive androgen receptor signaling inhibitors (ARSI), PARP inhibitors and other therapeutic regimes [22]. Similarly, Yazgan et al. found a pan-immune-inflammation value derived from total blood cell counts before treatment with ARSI with marked prognostic potential in patients with metastatic castration-resistant prostate cancer [24]. Regarding immunotherapy, PD-L1 is becoming quite popular as both genetic [25] and immunohistochemical [26] marker with prognostic and/or predictive roles

in renal cancer patients treated with immune checkpoint inhibitors. Finally, DNA damage response parameters are widely adopted for the prediction of response to certain treatment modalities in patients with advanced prostate cancer [27,28] or urothelial carcinoma [29]. However, there is a gap in knowledge regarding radiation-induced immune alterations which could serve as putative prognostic and/or predictive biomarkers in PCa.

RT, in addition to its direct tumoricidal effects, additionally exerts indirect antitumor effects via systemic immune activation resulting in an active immunosurveillance against non-irradiated tumor cells. The immune-activating effects of the ionizing radiation are thought to be primarily mediated via the release of tumor antigens from the dying tumor cells which act as an in situ vaccine for tumor peptide-specific T-cell priming [11]. Other immunopotentiating effects of RT include, but are not restricted to, M1 macrophage and T-cell accumulation into the tumor as well as the release of immunostimulatory adjuvants locally, all of which support the combination of RT with immunotherapy [30–34]. Clinical studies have also reported distant responses in patients receiving RT in combination with immune checkpoint inhibitors which were associated with alterations in circulating lymphocyte subsets and antibody responses to tumor-associated antigens [35–38]. In addition, there are studies to show changes in circulating immune cell subpopulations and cytokines in cancer patients after RT who did not receive systemic treatment [39,40]. However, so far there is no report to show an effect of RT on the expression of genes involved in immune regulation pathways affecting tumor progression which could further contribute to its immune-activating effects. Investigating differences in the expression of such genes in circulation post-RT could be critical for the design of novel immunotherapy trials in combination with RT.

The six critical genes, including *CCR7*, *FCGR2B*, *BTLA*, *CD6*, *CD3D* and *CD3E*, play important roles in favoring tumor progression and promoting negative immune-regulatory effects. For example, *CCR7* and its ligands (*CCL19/CCL21*) are a vital axis for carcinogenic properties, such as epithelial-mesenchymal transition, tumor invasion and migration [41,42]. In addition, high numbers of peripheral CD8+ T-cells expressing differentiation markers and lacking *CCR7* are associated with response to nivolumab in NSCLC patients [43] whereas the presence of CD8+*CCR7*+ T-cells in the peripheral blood has been demonstrated to associate with disease recurrences in patients with head and neck cancers [44]. Moreover, the silencing of *CCR7*, a protein involved in angiogenesis, inhibits prostate cancer cell proliferation, migration and invasion [45]. *FCGR2B* expressed by myeloid effector cells inhibits direct tumor cell depletion by therapeutic antibodies via competition with its activating FCGR counterparts. In addition, *FCGR2B* on malignant B-cells has been found to advance the internalization of targeting monoclonal antibodies, counteracting their capacity to generate antibody-dependent cellular cytotoxicity and thus diminishing their therapeutic efficacy [46]. Interestingly, in a melanoma mouse model, *FCGR2B* has been demonstrated to be upregulated in tumor-infiltrating CD8+ T-cells hampering their antitumor efficacy [47]. In the same study, it was also shown that CD8+ T-cells in melanoma patients express *FCGR2B*, proposing its role in down-regulating tumor-directed immune responses in humans. Increased levels of circulating *BTLA* or its high expression on CD8+ and CD4+ T-cell subsets have been reported to associate with poor prognosis in many types of malignant diseases [48–51]. More specifically, it has been shown that the reduction of *BTLA* expression in tumor infiltrating lymphocytes (TILs), through targeting *HVEM*, might result in better tumor control in a humanized mouse model of PCa [52]. Moreover, IFN γ production by tumor-specific CD8+ T-cells in response to melanocytic antigens has been shown to be impeded via *BTLA* signaling [53]. *CD6* functions as an immune checkpoint mainly expressed by lymphocytes including T and natural killer (NK) cells [54,55]. *CD6* interacts with its ligands on cancer cells restricting adaptive and innate antitumor immune responses [55]. Blocking this interaction with an anti-human *CD6* monoclonal antibody resulted in the enhanced killing of tumor cell lines in vitro by NK and CD8+ T-cells mostly via upregulation of the activating receptor *NKG2D* and increased expression levels of perforin/Granzyme B in parallel with a reduction of the inhibitory *NKG2A* receptor [55].

In the same study, it was shown that the blocking of CD6 in vivo resulted in the rapid rejection of breast cancer xenografts.

CD3D upregulation has been associated with resistance to anti-tumor therapy in patients with uveal melanoma, which was attributed to tumor infiltration by increased numbers of immune-suppressive regulatory T-cells [56]. The respective resistance mechanism involves the upregulation of indoleamine 2,3-dioxygenase and its interaction with $\text{IFN}\gamma$, leading to the promotion of tumor immunosuppression through regulatory T-cell-dependent recruitment of myeloid-derived suppressor cells [56,57]. Moreover, the downregulation of *CD3D* in the peripheral blood of PCa patients undergoing EBRT was correlated with CD8+ T-cell suppressed responses leading to the development of cancer-related fatigue during radiation therapy [58]. *CD3E* expression is upregulated in certain cancer types [59] and it has been recently highlighted as an attractive therapeutic target in cancer [60,61]. Preclinical studies in melanoma-bearing syngeneic mice revealed that the concomitant blockade of CD3E and TRP-1 facilitates tumor shrinkage through the enhanced influx of innate and adaptive immune cells [61]. A bioinformatics analysis using TCGA data from bladder cancer patients found *CD3E* to be downregulated in the luminal compared to basal tumor samples, with the luminal subtype being associated with better survival rates. In the same study, *CD3E* was highlighted as a substantial regulator of the tumor microenvironment, since CD4+ memory T-cells and regulatory T-cells were found to be negatively correlated with *CD3E* expression levels [60], while in low-grade glioma patients, *CD3E* upregulation served as a marker of significantly worse prognosis [62]. The possibility that downregulation of *CD3D* and *CD3E* genes post-RT could be attributed to an RT-based decreasing effect on circulating T-cell frequencies is unlikely since the blood sampling was performed at 3 months post-RT, by which time-point the lymphocyte numbers have been recovered to normal levels pre-RT [12,13].

PCa patients with localized disease receiving primary or adjuvant RT have an extended 5-years PFI which, as extrapolated from various studies, ranges between 90–100%, 80–95% and 60–87% for patients in the low-risk, intermediate-risk, and high-risk groups, respectively [18,19,63–66]. Consequently, it was not possible to do correlations with clinical outcomes because of the too short follow-up time (22–39 months) between the completion of RT and the writing of this manuscript. Therefore, we performed analyses in the PRAD dataset which revealed that below-median expression of the 6-GS mRNA was associated with a longer PFI over 5 years whereas a reduced PFI was seen in patients with above-median expression of the 6-GS. Notably, such correlations were found in groups of patients with poor clinicopathologic characteristics including Gleason score ≥ 8 and T-stage 3. Importantly, PFI for these patients with a high risk of recurrence having the favorable low expression 6-GS were almost indistinguishable from those observed in patients with more favorable clinicopathological parameters (i.e., Gleason score 7 and T-stage 2). We may propose that RT by lowering the expression of the 6-GS reinforces antitumor immunity resulting in slow tumor growth rates, thus increasing PFI. The possibility that the alterations in gene expression could be attributed to the ADT is highly unlikely simply due to the fact that all 23 PCa patients had been receiving ADT for 6 months before RT implying that these gene alterations should have been detected pre-RT. Nonetheless, we cannot formally exclude the possibility that such alterations could be the result of a combined effect among these two therapeutic modalities. This study has limitations due to the low number of patients examined and because it lacked experimental and clinical studies to validate the function of our 6 GS. With regard to the second limitation, the functional programme of these six genes could be extrapolated from the studies cited above, which demonstrate their role as critical components of various molecular pathways participating to the immune control of tumor progression. Regardless, more patients are needed to be examined along with further studies to substantiate the predictive value of this signature.

5. Conclusions

In conclusion, by comprehensively analyzing the immune gene expression levels in the peripheral blood of LPCa patients at baseline and post-RT, our study developed a model based on six genes related to immune suppression and tumor-promoting pathways. It is expected that the 6-GS will predict the prognosis of PCa patients not only with localized disease but also of patients at more advanced PCa stages.

Supplementary Materials: The following supporting information can be downloaded at: <https://www.mdpi.com/article/10.3390/cancers14205032/s1>, Table S1: Gene Ontology (GO) enrichment profiles, including the respective *p*-values and gene interconnections, of the 6-gene signature using the GOnet tool.

Author Contributions: Conceptualization, C.N.B.; Data curation, S.P.F., M.G., P.B. and S.S.; Formal analysis, S.P.F., M.G., N.A., P.B. and S.O.; Funding acquisition, C.N.B.; Investigation, S.P.F., M.G., P.B., D.C., G.M., S.S. and A.D.G.; Methodology, S.P.F., M.G. and S.S.; Project administration, C.N.B.; Resources, S.S., D.C., G.M. and C.N.B.; Supervision, C.N.B.; Validation, S.P.F., M.G., G.M. and C.N.B.; Visualization, S.P.F., M.G., N.A. and S.O.; Writing—original draft, S.P.F., M.G. and C.N.B.; Writing—review & editing, S.P.F., M.G., N.A., G.M., S.S., A.D.G. and C.N.B. All authors have read and agreed to the published version of the manuscript.

Funding: This research has been co-financed by the European Regional Development Fund of the European Union and Greek national funds through the Operational Program Competitiveness, Entrepreneurship and Innovation under the call RESEARCH—CREATE—INNOVATE (project code: T1EDK-01404). N.A. was supported by a doctoral fellowship from the Fondation Association pour la Recherche sur le Cancer (ARC).

Institutional Review Board Statement: The study was approved by the Saint Savas Cancer Hospital Institutional Review Board (approval no. IRB-ID6777/14-06-2017) and the Ethical Committee of the Medical School of the National and Kapodistrian University of Athens (approval no. ID247/28-01-2020).

Informed Consent Statement: Informed consent was obtained from all subjects involved in the study.

Data Availability Statement: The data presented in this study are available upon reasonable request.

Acknowledgments: The authors are grateful to all patients who participated in the present study.

Conflicts of Interest: The authors declare that they have no conflicts of interest.

References

1. Zhong, L.; Li, Y.; Xiong, L.; Wang, W.; Wu, M.; Yuan, T.; Yang, W.; Tian, C.; Miao, Z.; Wang, T.; et al. Small molecules in targeted cancer therapy: Advances, challenges, and future perspectives. *Signal Transduct. Target. Ther.* **2021**, *6*, 201. [\[CrossRef\]](#)
2. Waldman, A.D.; Fritz, J.M.; Lenardo, M.J. A guide to cancer immunotherapy: From T cell basic science to clinical practice. *Nat. Rev. Immunol.* **2020**, *20*, 651–668. [\[CrossRef\]](#)
3. Gross, S.; Rahal, R.; Stransky, N.; Lengauer, C.; Hoeflich, K.P. Targeting cancer with kinase inhibitors. *J. Clin. Invest.* **2015**, *125*, 1780–1789. [\[CrossRef\]](#)
4. Rawla, P. Epidemiology of Prostate Cancer. *World J. Oncol.* **2019**, *10*, 63–89. [\[CrossRef\]](#)
5. Podder, T.K.; Fredman, E.T.; Ellis, R.J. Advances in Radiotherapy for Prostate Cancer Treatment. *Adv. Exp. Med. Biol.* **2018**, *1096*, 31–47. [\[CrossRef\]](#)
6. Twyman-Saint Victor, C.; Rech, A.J.; Maity, A.; Rengan, R.; Pauken, K.E.; Stelekati, E.; Benci, J.L.; Xu, B.; Dada, H.; Odorizzi, P.M.; et al. Radiation and dual checkpoint blockade activate non-redundant immune mechanisms in cancer. *Nature* **2015**, *520*, 373–377. [\[CrossRef\]](#)
7. Vanpouille-Box, C.; Pilonis, K.A.; Wennerberg, E.; Formenti, S.C.; Demaria, S. In situ vaccination by radiotherapy to improve responses to anti-CTLA-4 treatment. *Vaccine* **2015**, *33*, 7415–7422. [\[CrossRef\]](#)
8. Carvalho, H.A.; Villar, R.C. Radiotherapy and immune response: The systemic effects of a local treatment. *Clinics* **2018**, *73*, e557s. [\[CrossRef\]](#)
9. Derer, A.; Deloch, L.; Rubner, Y.; Fietkau, R.; Frey, B.; Gaipl, U.S. Radio-Immunotherapy-Induced Immunogenic Cancer Cells as Basis for Induction of Systemic Anti-Tumor Immune Responses—Pre-Clinical Evidence and Ongoing Clinical Applications. *Front. Immunol.* **2015**, *6*, 505. [\[CrossRef\]](#)

10. Janopaul-Naylor, J.R.; Shen, Y.; Qian, D.C.; Buchwald, Z.S. The Abscopal Effect: A Review of Pre-Clinical and Clinical Advances. *Int. J. Mol. Sci.* **2021**, *22*, 11061. [[CrossRef](#)]
11. Baxevanis, C.N.; Gritzapis, A.D.; Voutsas, I.F.; Batsaki, P.; Goulielmaki, M.; Adamaki, M.; Zoumpourlis, V.; Fortis, S.P. T-Cell Repertoire in Tumor Radiation: The Emerging Frontier as a Radiotherapy Biomarker. *Cancers* **2022**, *14*, 2674. [[CrossRef](#)]
12. Wang, X.B.; Wu, D.J.; Chen, W.P.; Liu, J.; Ju, Y.J. Impact of radiotherapy on immunological parameters, levels of inflammatory factors, and clinical prognosis in patients with esophageal cancer. *J. Radiat. Res.* **2019**, *60*, 353–363. [[CrossRef](#)]
13. Eckert, F.; Schaedle, P.; Zips, D.; Schmid-Horch, B.; Rammensee, H.G.; Gani, C.; Gouttefangeas, C. Impact of curative radiotherapy on the immune status of patients with localized prostate cancer. *Oncoimmunology* **2018**, *7*, e1496881. [[CrossRef](#)]
14. Warde-Farley, D.; Donaldson, S.L.; Comes, O.; Zuberi, K.; Badrawi, R.; Chao, P.; Franz, M.; Grouios, C.; Kazi, F.; Lopes, C.T.; et al. The GeneMANIA prediction server: Biological network integration for gene prioritization and predicting gene function. *Nucleic Acids Res.* **2010**, *38*, W214–W220. [[CrossRef](#)]
15. Szklarczyk, D.; Franceschini, A.; Wyder, S.; Forslund, K.; Heller, D.; Huerta-Cepas, J.; Simonovic, M.; Roth, A.; Santos, A.; Tsafou, K.P.; et al. STRING v10: Protein–protein interaction networks, integrated over the tree of life. *Nucleic Acids Res.* **2015**, *43*, D447–D452. [[CrossRef](#)] [[PubMed](#)]
16. Pomazny, M.; Ha, B.; Peters, B. GOnet: A tool for interactive Gene Ontology analysis. *BMC Bioinform.* **2018**, *19*, 470. [[CrossRef](#)]
17. Tritschler, S.; Ganswindt, U.; Stief, C.G. Localized intermediate- to high-risk prostate cancer. *Urol. A* **2016**, *55*, 318–325. [[CrossRef](#)]
18. Potters, L.; Morgenstern, C.; Calugaru, E.; Fearn, P.; Jassal, A.; Presser, J.; Mullen, E. 12-year outcomes following permanent prostate brachytherapy in patients with clinically localized prostate cancer. *J. Urol.* **2005**, *173*, 1562–1566. [[CrossRef](#)]
19. Blasko, J.C.; Grimm, P.D.; Sylsvester, J.E.; Cavanagh, W. The role of external beam radiotherapy with I-125/Pd-103 brachytherapy for prostate carcinoma. *Radiother. Oncol.* **2000**, *57*, 273–278. [[CrossRef](#)]
20. Liu, Y.; Patel, S.A.; Jani, A.B.; Gillespie, T.W.; Patel, P.R.; Godette, K.D.; Hershatter, B.W.; Shelton, J.W.; McDonald, M.W. Overall Survival After Treatment of Localized Prostate Cancer with Proton Beam Therapy, External-Beam Photon Therapy, or Brachytherapy. *Clin. Genitourin. Cancer* **2021**, *19*, 255–266. [[CrossRef](#)]
21. Puche-Sanz, I.; Rodriguez-Martinez, A.; Garrido-Navas, M.C.; Robles-Fernandez, I.; Vazquez-Alonso, F.; Alvarez Cubero, M.J.; Lorente-Acosta, J.A.; Serrano-Fernandez, M.J.; Cozar-Olmo, J.M. Liquid biopsy and prostate cancer. Current evidence applied to clinical practice. *Actas Urol. Esp.* **2020**, *44*, 139–147. [[CrossRef](#)] [[PubMed](#)]
22. Casanova-Salas, I.; Athie, A.; Boutros, P.C.; Del Re, M.; Miyamoto, D.T.; Pienta, K.J.; Posadas, E.M.; Sowalsky, A.G.; Stenzl, A.; Wyatt, A.W.; et al. Quantitative and Qualitative Analysis of Blood-based Liquid Biopsies to Inform Clinical Decision-making in Prostate Cancer. *Eur. Urol.* **2021**, *79*, 762–771. [[CrossRef](#)] [[PubMed](#)]
23. De Kruijff, I.E.; Beijer, N.; Martens, J.W.M.; de Wit, R.; Boormans, J.L.; Sleijfer, S. Liquid Biopsies to Select Patients for Perioperative Chemotherapy in Muscle-invasive Bladder Cancer: A Systematic Review. *Eur. Urol. Oncol.* **2021**, *4*, 204–214. [[CrossRef](#)]
24. Yazgan, S.C.; Yekeduz, E.; Utkan, G.; Urun, Y. Prognostic role of pan-immune-inflammation value in patients with metastatic castration-resistant prostate cancer treated with androgen receptor-signaling inhibitors. *Prostate* **2022**, *82*, 1456–1461. [[CrossRef](#)] [[PubMed](#)]
25. Motzer, R.J.; Choueiri, T.K.; McDermott, D.F.; Powles, T.; Vano, Y.A.; Gupta, S.; Yao, J.; Han, C.; Ammar, R.; Papillon-Cavanagh, S.; et al. Biomarker analysis from CheckMate 214: Nivolumab plus ipilimumab versus sunitinib in renal cell carcinoma. *J. Immunother. Cancer* **2022**, *10*, e004316. [[CrossRef](#)] [[PubMed](#)]
26. Cimadamore, A.; Massari, F.; Santoni, M.; Lopez-Beltran, A.; Cheng, L.; Scarpelli, M.; Montironi, R.; Moch, H. PD1 and PD-L1 Inhibitors for the Treatment of Kidney Cancer: The Role of PD-L1 Assay. *Curr. Drug. Targets* **2020**, *21*, 1664–1671. [[CrossRef](#)]
27. Mateo, J.; Carreira, S.; Sandhu, S.; Miranda, S.; Mossop, H.; Perez-Lopez, R.; Nava Rodrigues, D.; Robinson, D.; Omlin, A.; Tunariu, N.; et al. DNA-Repair Defects and Olaparib in Metastatic Prostate Cancer. *N Engl. J. Med.* **2015**, *373*, 1697–1708. [[CrossRef](#)]
28. Cattrini, C.; Espana, R.; Mennitto, A.; Bersanelli, M.; Castro, E.; Olmos, D.; Lorente, D.; Gennari, A. Optimal Sequencing and Predictive Biomarkers in Patients with Advanced Prostate Cancer. *Cancers* **2021**, *13*, 4522. [[CrossRef](#)]
29. Claps, F.; Mir, M.C.; Zargar, H. Molecular markers of systemic therapy response in urothelial carcinoma. *Asian J. Urol.* **2021**, *8*, 376–390. [[CrossRef](#)]
30. Apetoh, L.; Ghiringhelli, F.; Tesniere, A.; Obeid, M.; Ortiz, C.; Criollo, A.; Mignot, G.; Maiuri, M.C.; Ullrich, E.; Saulnier, P.; et al. Toll-like receptor 4-dependent contribution of the immune system to anticancer chemotherapy and radiotherapy. *Nat. Med.* **2007**, *13*, 1050–1059. [[CrossRef](#)]
31. Obeid, M.; Tesniere, A.; Ghiringhelli, F.; Fimia, G.M.; Apetoh, L.; Perfettini, J.L.; Castedo, M.; Mignot, G.; Panaretakis, T.; Casares, N.; et al. Calreticulin exposure dictates the immunogenicity of cancer cell death. *Nat. Med.* **2007**, *13*, 54–61. [[CrossRef](#)] [[PubMed](#)]
32. Lee, Y.; Auh, S.L.; Wang, Y.; Burnette, B.; Wang, Y.; Meng, Y.; Beckett, M.; Sharma, R.; Chin, R.; Tu, T.; et al. Therapeutic effects of ablative radiation on local tumor require CD8+ T cells: Changing strategies for cancer treatment. *Blood* **2009**, *114*, 589–595. [[CrossRef](#)] [[PubMed](#)]
33. Klug, F.; Prakash, H.; Huber, P.E.; Seibel, T.; Bender, N.; Halama, N.; Pfirschke, C.; Voss, R.H.; Timke, C.; Umansky, L.; et al. Low-dose irradiation programs macrophage differentiation to an iNOS(+)/M1 phenotype that orchestrates effective T cell immunotherapy. *Cancer Cell* **2013**, *24*, 589–602. [[CrossRef](#)]
34. Wu, C.Y.; Yang, L.H.; Yang, H.Y.; Knoff, J.; Peng, S.; Lin, Y.H.; Wang, C.; Alvarez, R.D.; Pai, S.I.; Roden, R.B.; et al. Enhanced cancer radiotherapy through immunosuppressive stromal cell destruction in tumors. *Clin. Cancer Res.* **2014**, *20*, 644–657. [[CrossRef](#)] [[PubMed](#)]

35. Mukherjee, A.G.; Wanjari, U.R.; Prabakaran, D.S.; Ganesan, R.; Renu, K.; Dey, A.; Vellingiri, B.; Kandasamy, S.; Ramesh, T.; Gopalakrishnan, A.V. The Cellular and Molecular Immunotherapy in Prostate Cancer. *Vaccines* **2022**, *10*, 1370. [[CrossRef](#)]
36. Lindner, D.; Arndt, C.; Loureiro, L.R.; Feldmann, A.; Kegler, A.; Koristka, S.; Berndt, N.; Mitwasi, N.; Bergmann, R.; Frenz, M.; et al. Combining Radiation- with Immunotherapy in Prostate Cancer: Influence of Radiation on T Cells. *Int. J. Mol. Sci.* **2022**, *23*, 7922. [[CrossRef](#)]
37. Sharabi, A.B.; Lim, M.; DeWeese, T.L.; Drake, C.G. Radiation and checkpoint blockade immunotherapy: Radiosensitisation and potential mechanisms of synergy. *Lancet Oncol.* **2015**, *16*, e498–e509. [[CrossRef](#)]
38. Crittenden, M.; Kohrt, H.; Levy, R.; Jones, J.; Camphausen, K.; Dicker, A.; Demaria, S.; Formenti, S. Current clinical trials testing combinations of immunotherapy and radiation. *Semin. Radiat. Oncol.* **2015**, *25*, 54–64. [[CrossRef](#)]
39. D’Auria, F.; Statuto, T.; Rago, L.; Montagna, A.; Castaldo, G.; Schiro, I.; Zeccola, A.; Virgilio, T.; Bianchino, G.; Traficante, A.; et al. Modulation of Peripheral Immune Cell Subpopulations After RapidArc/Moderate Hypofractionated Radiotherapy for Localized Prostate Cancer: Findings and Comparison With 3D Conformal/Conventional Fractionation Treatment. *Front. Oncol.* **2022**, *12*, 829812. [[CrossRef](#)]
40. McGee, H.M.; Daly, M.E.; Azghadi, S.; Stewart, S.L.; Oesterich, L.; Schlom, J.; Donahue, R.; Schoenfeld, J.D.; Chen, Q.; Rao, S.; et al. Stereotactic Ablative Radiation Therapy Induces Systemic Differences in Peripheral Blood Immunophenotype Dependent on Irradiated Site. *Int. J. Radiat. Oncol. Biol. Phys.* **2018**, *101*, 1259–1270. [[CrossRef](#)]
41. Chen, Y.; Shao, Z.; Jiang, E.; Zhou, X.; Wang, L.; Wang, H.; Luo, X.; Chen, Q.; Liu, K.; Shang, Z. CCL21/CCR7 interaction promotes EMT and enhances the stemness of OSCC via a JAK2/STAT3 signaling pathway. *J. Cell Physiol.* **2020**, *235*, 5995–6009. [[CrossRef](#)] [[PubMed](#)]
42. Korbecki, J.; Grochans, S.; Gutowska, I.; Barczak, K.; Baranowska-Bosiacka, I. CC Chemokines in a Tumor: A Review of Pro-Cancer and Anti-Cancer Properties of Receptors CCR5, CCR6, CCR7, CCR8, CCR9, and CCR10 Ligands. *Int. J. Mol. Sci.* **2020**, *21*, 7619. [[CrossRef](#)]
43. Kunert, A.; Basak, E.A.; Hurkmans, D.P.; Balcioglu, H.E.; Klaver, Y.; van Brakel, M.; Oostvogels, A.A.M.; Lamers, C.H.J.; Bins, S.; Koolen, S.L.W.; et al. CD45RA(+)CCR7(-) CD8 T cells lacking co-stimulatory receptors demonstrate enhanced frequency in peripheral blood of NSCLC patients responding to nivolumab. *J. Immunother. Cancer* **2019**, *7*, 149. [[CrossRef](#)] [[PubMed](#)]
44. Czystowska, M.; Gooding, W.; Szczepanski, M.J.; Lopez-Abaitero, A.; Ferris, R.L.; Johnson, J.T.; Whiteside, T.L. The immune signature of CD8(+)CCR7(+) T cells in the peripheral circulation associates with disease recurrence in patients with HNSCC. *Clin. Cancer Res.* **2013**, *19*, 889–899. [[CrossRef](#)] [[PubMed](#)]
45. Chi, B.J.; Du, C.L.; Fu, Y.F.; Zhang, Y.N.; Wang, R.W. Silencing of CCR7 inhibits the growth, invasion and migration of prostate cancer cells induced by VEGFC. *Int. J. Clin. Exp. Pathol.* **2015**, *8*, 12533–12540.
46. Lim, S.H.; Vaughan, A.T.; Ashton-Key, M.; Williams, E.L.; Dixon, S.V.; Chan, H.T.; Beers, S.A.; French, R.R.; Cox, K.L.; Davies, A.J.; et al. Fc gamma receptor IIIb on target B cells promotes rituximab internalization and reduces clinical efficacy. *Blood* **2011**, *118*, 2530–2540. [[CrossRef](#)]
47. Farley, C.R.; Morris, A.B.; Tariq, M.; Bennion, K.B.; Potdar, S.; Kudchadkar, R.; Lowe, M.C.; Ford, M.L. FcgammaRIIB is a T cell checkpoint in antitumor immunity. *JCI Insight* **2021**, *6*, e135623. [[CrossRef](#)]
48. Malissen, N.; Macagno, N.; Granjeaud, S.; Granier, C.; Moutardier, V.; Gaudy-Marqueste, C.; Habel, N.; Mandavit, M.; Guillot, B.; Pasero, C.; et al. HVEM has a broader expression than PD-L1 and constitutes a negative prognostic marker and potential treatment target for melanoma. *Oncoimmunology* **2019**, *8*, e1665976. [[CrossRef](#)]
49. Migita, K.; Sho, M.; Shimada, K.; Yasuda, S.; Yamato, I.; Takayama, T.; Matsumoto, S.; Wakatsuki, K.; Hotta, K.; Tanaka, T.; et al. Significant involvement of herpesvirus entry mediator in human esophageal squamous cell carcinoma. *Cancer* **2014**, *120*, 808–817. [[CrossRef](#)]
50. Lan, X.; Li, S.; Gao, H.; Nanding, A.; Quan, L.; Yang, C.; Ding, S.; Xue, Y. Increased BTLA and HVEM in gastric cancer are associated with progression and poor prognosis. *Onco. Targets Ther.* **2017**, *10*, 919–926. [[CrossRef](#)]
51. Hokuto, D.; Sho, M.; Yamato, I.; Yasuda, S.; Obara, S.; Nomi, T.; Nakajima, Y. Clinical impact of herpesvirus entry mediator expression in human hepatocellular carcinoma. *Eur. J. Cancer* **2015**, *51*, 157–165. [[CrossRef](#)] [[PubMed](#)]
52. Aubert, N.; Brunel, S.; Olive, D.; Marodon, G. Blockade of HVEM for Prostate Cancer Immunotherapy in Humanized Mice. *Cancers* **2021**, *13*, 3009. [[CrossRef](#)] [[PubMed](#)]
53. Derre, L.; Rivals, J.P.; Jandus, C.; Pastor, S.; Rimoldi, D.; Romero, P.; Michielin, O.; Olive, D.; Speiser, D.E. BTLA mediates inhibition of human tumor-specific CD8+ T cells that can be partially reversed by vaccination. *J. Clin. Invest.* **2010**, *120*, 157–167. [[CrossRef](#)] [[PubMed](#)]
54. Brown, M.H. CD6 as a Cell Surface Receptor and As a Target for Regulating Immune Responses. *Curr. Drug. Targets* **2016**, *17*, 619–629. [[CrossRef](#)]
55. Ruth, J.H.; Gurrea-Rubio, M.; Athukorala, K.S.; Rasmussen, S.M.; Weber, D.P.; Randon, P.M.; Gedert, R.J.; Lind, M.E.; Amin, M.A.; Campbell, P.L.; et al. CD6 is a target for cancer immunotherapy. *JCI Insight* **2021**, *6*, e145662. [[CrossRef](#)]
56. Liang, C.; Peng, L.; Zeng, S.; Zhao, Q.; Tang, L.; Jiang, X.; Zhang, J.; Yan, N.; Chen, Y. Investigation of indoleamine 2,3-dioxygenase 1 expression in uveal melanoma. *Exp. Eye Res.* **2019**, *181*, 112–119. [[CrossRef](#)]
57. Holmgaard, R.B.; Zamarin, D.; Li, Y.; Gasmir, B.; Munn, D.H.; Allison, J.P.; Merghoub, T.; Wolchok, J.D. Tumor-Expressed IDO Recruits and Activates MDSCs in a Treg-Dependent Manner. *Cell Rep.* **2015**, *13*, 412–424. [[CrossRef](#)]

58. Saligan, L.N.; Lukkahatai, N.; Zhang, Z.J.; Cheung, C.W.; Wang, X.M. Altered Cd8+ T lymphocyte Response Triggered by Arginase 1: Implication for Fatigue Intensification during Localized Radiation Therapy in Prostate Cancer Patients. *Neuropsychiatry* **2018**, *8*, 1249–1262. [[CrossRef](#)]
59. Gaffney, S.G.; Perry, E.B.; Chen, P.M.; Greenstein, A.; Kaech, S.M.; Townsend, J.P. The landscape of novel and complementary targets for immunotherapy: An analysis of gene expression in the tumor microenvironment. *Oncotarget* **2019**, *10*, 4532–4545. [[CrossRef](#)]
60. Liu, Y.; Wu, Y.; Zhang, P.; Xu, C.; Liu, Z.; He, C.; Liu, Y.; Kang, Z. CXCL12 and CD3E as Indicators for Tumor Microenvironment Modulation in Bladder Cancer and Their Correlations with Immune Infiltration and Molecular Subtypes. *Front. Oncol.* **2021**, *11*, 636870. [[CrossRef](#)]
61. Benonisson, H.; Altintas, I.; Sluijter, M.; Verploegen, S.; Labrijn, A.F.; Schuurhuis, D.H.; Houtkamp, M.A.; Verbeek, J.S.; Schuurman, J.; van Hall, T. CD3-Bispecific Antibody Therapy Turns Solid Tumors into Inflammatory Sites but Does Not Install Protective Memory. *Mol. Cancer Ther.* **2019**, *18*, 312–322. [[CrossRef](#)] [[PubMed](#)]
62. Lu, X.; Li, C.; Xu, W.; Wu, Y.; Wang, J.; Chen, S.; Zhang, H.; Huang, H.; Huang, H.; Liu, W. Malignant Tumor Purity Reveals the Driven and Prognostic Role of CD3E in Low-Grade Glioma Microenvironment. *Front. Oncol.* **2021**, *11*, 676124. [[CrossRef](#)] [[PubMed](#)]
63. Snyder, K.M.; Stock, R.G.; Hong, S.M.; Lo, Y.C.; Stone, N.N. Defining the risk of developing grade 2 proctitis following 125I prostate brachytherapy using a rectal dose-volume histogram analysis. *Int. J. Radiat. Oncol. Biol. Phys.* **2001**, *50*, 335–341. [[CrossRef](#)]
64. Deutsch, I.; Zelefsky, M.J.; Zhang, Z.; Mo, Q.; Zaider, M.; Cohen, G.; Cahlon, O.; Yamada, Y. Comparison of PSA relapse-free survival in patients treated with ultra-high-dose IMRT versus combination HDR brachytherapy and IMRT. *Brachytherapy* **2010**, *9*, 313–318. [[CrossRef](#)]
65. Ishiyama, H.; Satoh, T.; Kitano, M.; Tabata, K.; Komori, S.; Ikeda, M.; Soda, I.; Kurosaka, S.; Sekiguchi, A.; Kimura, M.; et al. High-dose-rate brachytherapy and hypofractionated external beam radiotherapy combined with long-term hormonal therapy for high-risk and very high-risk prostate cancer: Outcomes after 5-year follow-up. *J. Radiat. Res.* **2014**, *55*, 509–517. [[CrossRef](#)]
66. Makino, T.; Mizokami, A.; Namiki, M. Clinical outcomes of patients with localized and locally advanced prostate cancer undergoing high-dose-rate brachytherapy with external-beam radiotherapy at our institute. *Anticancer Res.* **2015**, *35*, 1723–1728.